

# Stochastic Investment Planning model of Multi-energy Microgrids considering Network Operational Uncertainties

Ali Ehsan, Qiang Yang, *Senior Member, IEEE*

**Abstract**—This work proposes a scenario-based stochastic microgrid investment planning model in the presence of various forms of generation and demand with operational uncertainties. The solution aims to minimize the overall cost and carbon dioxide emissions in microgrid through determining the optimal placement and capacities (i.e. siting and sizing) of the distributed energy resources (DERs). The DER mix comprises of the wind turbines, photovoltaics, gas-boiler, and combined heat and power units. The proposed planning model is based on linear power flow and heat transfer equations, and explicitly captures the interaction between electricity and heating DERs. To address the operational uncertainties associated with the wind and photovoltaic generation as well as the electricity and heating demands, an uncertainty matrix is adopted. The uncertainty matrix is generated using the heuristic moment matching (HMM) method that effectively captures the stochastic moments and correlation among the historical data. The numerical results from a case-study on 19-bus microgrid test system confirm the effectiveness of the proposed model.

**Index Terms**—microgrid; distributed energy resource; heuristic moment matching; operational uncertainties.

## NOMENCLATURE

### Indices and Sets

$c$	Set of continuous distributed energy resources (DERs): photovoltaic (pv), Gas boiler (bl)
$d$	Set of discrete DERs: wind turbine (wt), CHP-internal combustion engine (ice)
$g$	Set of all distributed energy resources ( $c \cup d$ )
$l$	Set of loads: electricity (el), heating (hl)
$h / \Omega^H$	Index/set of generated scenarios
$i / \Omega^B$	Index/set of buses
$i - j / \Omega^L$	Index/set of branches

### Parameters

$\alpha_{chp}$	Heat-to-power recovery ratio of CHP-ICE
$\gamma_{ij}$	Heat loss coefficient for heat transfer pipe $i-j$ (% per meter)
$\lambda_{i,i-j}$	Correlation factor of $i^{th}$ bus and branch $i-j$

This work is supported in part by the National Natural Science Foundation of China (51777183) and the Natural Science Foundation of Zhejiang Province (LZ15E070001). A. Ehsan and Q. Yang are with College of Electrical Engineering, Zhejiang University, China (Corresponding author e-mail: qyang@zju.edu.cn).

$ar^g$	Annuity rate for $g^{th}$ DER
$c^u$	Penalty cost of unsupplied loads (\$/MW)
$cc^d$	Capital cost of discrete DER (\$/MW)
$ec^g$	Emissions rate for $g^{th}$ DER (kg/MWh)
$fc^c, vc^c$	Fixed capital cost (\$) and variable capital cost (\$/MW) of continuous DER
$\bar{h}_{ij}$	Heat transfer capacity for pipe $i-j$ (MW)
$\underline{I}, \bar{I}$	Lower & upper limit on branch current
$N_h, N_y$	Number of scenarios and hours of a year
$oc^g$	Operation cost of $g^{th}$ DER (\$/MWh)
$\bar{p}_i^d$	Maximum operating power of discrete DER at $i^{th}$ bus (MW)
$r_{ij}, x_{ij}$	Resistance and reactance of branch $i-j$
$\underline{v}, \bar{v}$	Lower and upper limit on bus voltage

### Variables and Functions

$b_c^i$	Binary variable for continuous DER at $i^{th}$ bus
$C_{cost}$	Overall microgrid costs
$C_{CO_2}$	Overall microgrid CO <sub>2</sub> emissions
$h_{ij,h}$	Heat flow in pipe $i-j$ for scenario $h$ (MW)
$I_{ij,h}$	Current in branch $i-j$ for scenario $h$
$n_d^i$	Number of discrete DERs at $i^{th}$ bus
$P_{ij,h}, Q_{ij,h}$	Active and reactive power flow in branch $i-j$ for scenario $h$ (MW)
$P_{i,h}^g, Q_{i,h}^g$	Active and reactive power output of $g^{th}$ DER at $i^{th}$ bus for scenario $h$ (MW)
$P_c^i$	Continuous DER capacity at $i^{th}$ bus (MW)
$P_i^l, Q_i^l$	Active/reactive load at $i^{th}$ bus (MW)
$P_{i,h}^l, Q_{i,h}^l$	Active/reactive load at $i^{th}$ bus for scenario $h$ (MW)
$P_i^{pv}, Q_i^{pv}$	Rated active and reactive power capacity of photovoltaic at $i^{th}$ bus (MW)
$P_{i,h}^{pv}, Q_{i,h}^{pv}$	Active and reactive power output of photovoltaic at $i^{th}$ bus for scenario $h$ (MW)
$P_{i,h}^u$	Unsupplied loads at $i^{th}$ bus for scenario $h$ (MW)
$P_i^{wt}, Q_i^{wt}$	Rated active and reactive power capacity of wind turbine at $i^{th}$ bus (MW)
$P_{i,h}^{wt}, Q_{i,h}^{wt}$	Active and reactive power output of wind turbine at $i^{th}$ bus for scenario $h$ (MW)
$v_{i,h}$	Voltage at $i^{th}$ bus for scenario $h$

## I. INTRODUCTION

TO ensure the security of power supply and mitigation of carbon emissions, conventional microgrids (MGs) are transitioning to renewable based multi-energy microgrids [1]. Such microgrids offer several benefits, in terms of renewable integration, low carbon dioxide emissions, in addition to the security and economy of power supply. However, this transition is accompanied by the uncertainties of intermittent renewable distributed energy resources (DERs), i.e. wind turbines (WTs) and photovoltaics (PVs). Thus, advanced network planning tools are required to explicitly address such operational uncertainties introduced to the microgrid network [2], and efficiently model the interaction between electricity and heating DERs in the multi-energy microgrids [1].

In the existing literature, the MG planning models in [3], [4] studied the electrical energy flows in the microgrid, but the energy flows of heating and cooling were not considered. Similarly, the planning techniques in [5], [6] investigated the supply and demand of electricity in the distribution network with a restricted DER mix. A few works [7]–[10] investigated the planning of multi-energy microgrid considering the electricity and heating demands. The authors in [7], studied the optimal allocation of an electricity and heating DER mix, however, electrical energy was modeled as a commodity, and the power flow constraints were neglected. Similarly, the DER planning methods in [8], [9] ignored the power flow equations. In [1], [10], both electrical and thermal networks were modeled for the optimal allocation of combined heat and power (CHP) and renewable DERs. However, the nonlinear formulation in [10] is solved via a stochastic technique, which is not computationally efficient. In addition, the uncertainties of renewable generation and load demand were not investigated in [1].

To address the aforementioned technical challenges, this work proposes a scenario-based stochastic multi-energy microgrid investment planning (MMIP) model. The proposed planning approach utilizes linear power flow and heat transfer equations to model the interplay between electricity and heating DERs. The main technical contributions made in this work are: (1) The operational uncertainties associated with WT generation, PV generation and electricity/heating demand are explicitly modelled via an uncertainty matrix, using the heuristic moment matching (HMM) method; and (2) the uncertainty matrix is incorporated to formulate the scenario-based stochastic MMIP model to determine the optimal siting and sizing of electricity and heating DERs to minimize the overall microgrid cost and CO<sub>2</sub> emissions.

The rest of the work is organized as follows: Section II presents the modeling of multi-energy microgrid and HMM-based uncertainty matrix, along with the formulation of proposed MMIP problem; Section III presents and discusses the numerical results; and finally, Section IV presents the conclusion and future work.

## II. THE PROPOSED APPROACH

The framework of the scenario-based stochastic MMIP model is summarized in Fig. 1. Firstly, the uncertainty matrix comprising of the representative scenarios for WT/PV generation and electricity/heating demand is generated using the HMM method [11]. Then, the uncertainty matrix is incorporated to formulate the proposed MMIP problem using YALMIP modelling language [12]. Finally, the MMIP problem is solved in CPLEX-MATLAB interface [13].

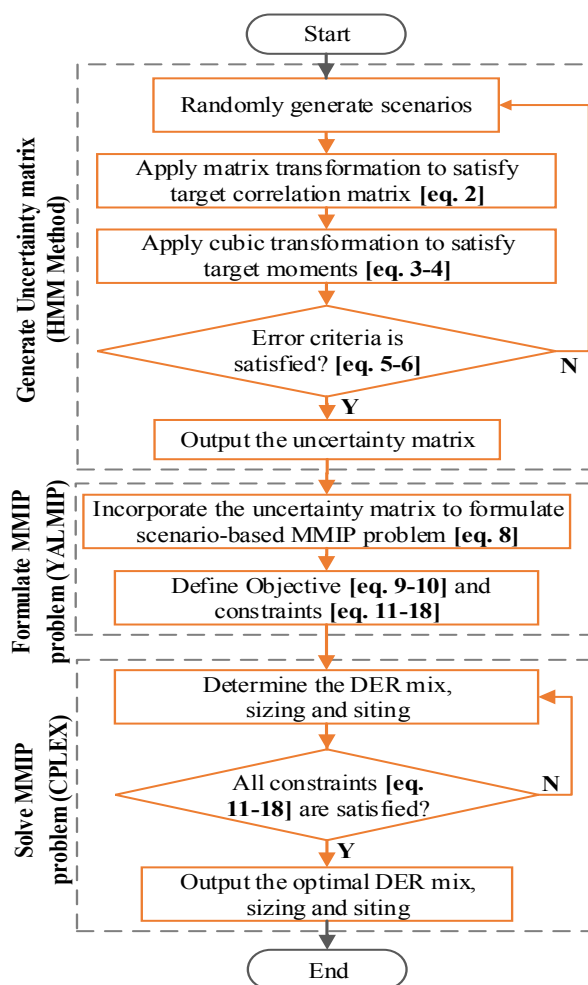


Fig. 1. Framework of multi-energy microgrid investment planning model

### A. Multi-energy Microgrid Model

The multi-energy microgrid model is shown in Fig. 2. The electricity demand is supplied by a mix of CHP-enabled internal combustion engines (ICE), wind turbines and photovoltaics. The heating demand (i.e. space and water heating) is delivered by a mix of the gas-fired boilers and recovered heat from CHP-ICE. The association between electricity and heating dispatch in the microgrid is made possible by the consideration of CHP recovered heat. In this work, continuous variables are used to model the optimal capacities of DERs available in small-scale modules, hereby called the continuous DERs, i.e. PV and boiler. Discrete variables are used for the rest of the DERs, hereby called the discrete DERs, i.e. WT and CHP-ICE.

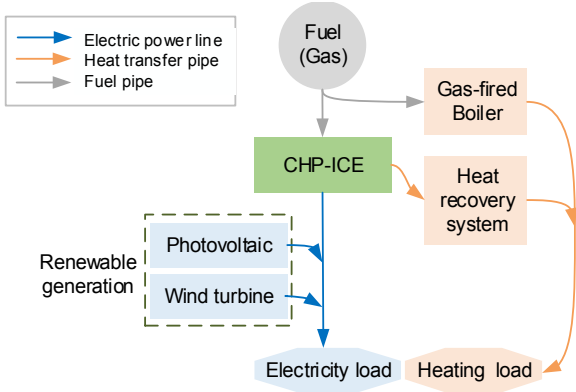


Fig. 2. Multi-energy microgrid system model

### B. Scenario Modeling

The uncertainty matrix is modeled via the HMM method [11], which captures the stochastic moments (i.e. expectation, standard deviation, skewness, and kurtosis) and correlation among the historical data. Firstly, the target moments and target correlation matrix ( $R$ ) of the historical hourly WT/PV generation and demand are determined, and normalized [11], as given in (1), where  $M_{i,k}^{NT}$  and  $M_{i,k}^T$  are the  $k^{\text{th}}$  normalized moment and  $k^{\text{th}}$  target moment of  $i^{\text{th}}$  column vector, respectively. In (1),  $k=1,2,3,4$  refer to expectation, standard deviation, skewness and kurtosis, respectively, while  $i=1,2,3,4$  refer to WT generation, PV generation, electricity load and heating load, respectively. Then,  $N_h$  scenarios of  $N_u$  uncertainty factors, i.e. WT generation ( $X_1$ ), PV generation ( $X_2$ ), electricity load ( $X_3$ ) and heating load ( $X_4$ ) are randomly produced to obtain the  $n$ -dimensional random matrix  $\mathbf{X}_{N_h \times N_u}$  [11]. Then, matrix transformation [11], as given in (2), is applied to convert  $\mathbf{X}_{N_h \times N_u}$  into the  $n$ -dimensional matrix  $\mathbf{Y}_{N_h \times N_u}$  to satisfy  $R$ , where  $L$  is the lower-triangle matrix of  $R$  determined via Cholesky decomposition. Then, cubic transformation [11], as given in (3), transforms  $\mathbf{Y}_{N_h \times N_u}$  into  $n$ -dimensional matrix of normalized scenarios  $\mathbf{Z}_{N_h \times N_u}$  to satisfy  $M_{i,k}^{NT}$ .  $a_i, b_i, c_i, d_i$  in (3) are calculated assuming that the moments of target scenarios ( $M_{i,k}(\mathbf{Z}_i)$ ) are equal to  $M_{i,k}^T$ , as given in (4). The solution converges when the moment error ( $\varepsilon_m$ ) and correlation error ( $\varepsilon_c$ ), as given in (5) and (6), respectively, are less than predefined thresholds, i.e.  $\overline{\varepsilon}_m = 5\%$ ,  $\overline{\varepsilon}_c = 5\%$ .

$M_{ik}^G$  in (5) is the  $k^{\text{th}}$  moment of  $i^{\text{th}}$  generated column vector  $\mathbf{Z}_i$ . In (6),  $R_{il}^G$  is correlation matrix of generated scenarios and  $R_{il}^{NT}$  is target correlation matrix of historical scenarios. Lastly,  $\mathbf{Z}_{N_h \times N_u}$  is inverted to satisfy  $M_{i,k}^T$ , resulting in the uncertainty matrix  $\mathbf{\Omega}^H = [P_h^{wt}, P_h^{pv}, P_h^{el}, P_h^{hl}]$ , containing

scenarios of WT generation ( $P_h^{wt}$ ), PV generation ( $P_h^{pv}$ ), electricity load ( $P_h^{el}$ ) and heating load ( $P_h^{hl}$ ), as given in (7).

$$\begin{cases} M_{i,1}^{NT} = 0, & M_{i,2}^{NT} = 1 \\ M_{i,3}^{NT} = \frac{M_{i,3}^T}{(\sqrt{M_{i,2}^T})^3}, & M_{i,4}^{NT} = \frac{M_{i,4}^T}{(M_{i,2}^T)^4} \end{cases} \quad (1)$$

$$\begin{cases} \mathbf{Y} = \mathbf{L} \times \mathbf{X} = \sum_{j=1}^i \mathbf{L}_{ij} \times \mathbf{X}_j \\ \mathbf{R} = \mathbf{L}\mathbf{L}^T \end{cases} \quad (2)$$

$$\mathbf{Z}_i = a_i + b_i \mathbf{Y}_i + c_i \mathbf{Y}_i^2 + d_i \mathbf{Y}_i^3 \quad (3)$$

$$M_{i,k}(\mathbf{Z}_i) = M_{i,k}^T \quad (4)$$

$$\varepsilon_m = \sum_{i=1}^{N_h} \left( \left| M_{i1}^G - M_{i1}^{NT} \right| + \sum_{k=2}^4 \left| M_{ik}^G - M_{ik}^{NT} \right| / M_{ik}^{NT} \right) \quad (5)$$

$$\varepsilon_c = \sum_{i=1}^{N_h} \sqrt{\frac{2}{N_u(N_u-1)} \sum_{i=1}^{N_u} \sum_{i=1}^{N_u} (R_{il}^G - R_{il}^{NT})^2} \quad (6)$$

$$\mathbf{\Omega}^H = \sqrt{M_{i,2}^T} \times \mathbf{Z}_i + M_{i,3}^{NT} \quad (7)$$

### C. Problem Formulation

To capture the network uncertainties, the uncertainty matrix is integrated with the deterministic decision variables ( $P_i^{wt}, P_i^{pv}, P_i^{el}, P_i^{hl}$ ), as given in (8). The objective of the proposed MMIP problem is to minimize the overall microgrid costs and CO<sub>2</sub> emissions over the planning horizon, under all scenarios. The overall costs objective in (9) accounts for the annualized investment cost of discrete and continuous DERs (where annuity rate depends on interest rate and DER lifetime), the operation cost and the cost of unsupplied loads. The CO<sub>2</sub> emissions objective in (10) considers the CO<sub>2</sub> emissions from the operation of all DERs. As suggested in [1], the operation costs and emissions in (1) and (2), respectively, are scaled up from  $H$ -scenarios to 8760 hours of a year using the weight factor ( $w = N_y / N_h$ ).

$$\begin{cases} P_{i,h}^{g \in \{wt, pv\}} = P_i^{g \in \{wt, pv\}} \times P_h^{g \in \{wt, pv\}} \\ P_{i,h}^{l \in \{el, hl\}} = P_i^{l \in \{el, hl\}} \times P_h^{l \in \{el, hl\}} \end{cases} \quad (8)$$

$$C_{\text{cost}} = \sum_{i,c} n_i^d \cdot \overline{P_i^d} \cdot cc^d \cdot ar^d + \sum_{i,d} (fc^c \cdot b_i^c + vc^c \cdot P_i^c) \cdot ar^c + \frac{N_y}{N_h} \sum_{i,g,h} P_{i,h}^g \cdot oc^g + \frac{N_y}{N_h} \sum_{i,h} P_{i,h}^u \cdot c^u \quad (9)$$

$$C_{CO_2} = \frac{N_y}{N_h} \sum_{i,g,h} P_{i,h}^g \cdot ec^g \quad (10)$$

The objectives in (9) and (10) are subject to the following electricity and heating network constraints. The electricity network security constraints (11)-(16) adopt the mixed-integer quadratically constrained programming based convex power flow model [14]. Constraint (11) balances the total active power generation of WT, PV and CHP against the load at each bus. Constraint (12) ensures the nodal power

balance for the total reactive power generation and load. Constraints (13) and (14) define the bus voltage and branch current, respectively, in terms of active and reactive power flows. Constraints (15) and (16) restrict the bus voltage and branch current, respectively.

$$\sum_{i-j \in \Omega^L} (\lambda_{i,j} P_{ij,h}) + \sum_{g \in \{wt, pv, chp\}} P_{i,h}^g + P_{i,h}^u = P_{ij,h}^{loss} + P_{i,h}^{l-el} \quad (11)$$

$$\sum_{i-j \in \Omega^L} (\lambda_{i,j} Q_{ij,h}) + \sum_{g \in \{wt, pv, chp\}} Q_{i,h}^g + Q_{i,h}^u = Q_{i,h}^{loss} + Q_{i,h}^{l-el} \quad (12)$$

$$v_{j,h}^2 = v_{i,h}^2 - 2(r_{ij} p_{ij,h} + x_{ij} q_{ij,h}) + (r_{ij}^2 + x_{ij}^2) I_{ij,h}^2 \quad (13)$$

$$v_{i,h}^2 I_{ij,h}^2 \geq P_{ij,h}^2 + Q_{ij,h}^2 \quad (14)$$

$$\underline{v} \leq v_{i,h} \leq \bar{v} \quad (15)$$

$$|I_{ij,h}| \leq \bar{I} \quad (16)$$

The heat balance constraint (17) accounts for the boiler heat, recovered heat from CHP, heating loads, and heat transfer through the piping network considering losses, at each bus [1]. Equation (18) restricts the heat pipe capacities.

$$\sum_{i-j \in \Omega^L} (\lambda_{i,j} h_{ij,h}) + P_{i,h}^{g=bl} + \alpha_{chp} P_{i,h}^{g=chp} = P_{i,h}^{l=hl} + \sum_{i-j \in \Omega^L} \gamma_{ij} h_{ij,h} \quad (17)$$

$$0 \leq h_{ij,h} \leq \bar{h}_{ij} \quad (18)$$

### III. NUMERICAL RESULTS AND DISCUSSION

#### A. Case Study Setup

Two cases with different objectives are considered. Firstly, Case I minimizes the overall microgrid costs, as given in (9). Secondly, Case II minimizes the composite objective (i.e. 50% weight for costs objective and 50% weight for emissions objective, as given in (9) and (10), respectively). The 19-bus island microgrid [1] (Fig. 4) with a radial electricity and heat piping network is considered. The load at each bus consists of the electricity and heating demand. All buses are considered candidate for DER placement. The investment parameters for the continuous and discrete DERs are given in Table I and II, respectively [15], [16].

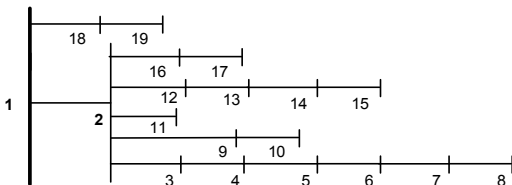


Fig. 3. Topology of the 19-bus multi-energy microgrid

TABLE I  
INVESTMENT PARAMETERS FOR CONTINUOUS DERs

Item	Photovoltaic	Gas Boiler
Fixed cost (M\$)	0.0025	0.0060
Variable cost (M\$/MW)	2.5	0.045
Operation cost (M\$/MWh)	0.000040	0.0001
Lifetime (years)	20	10
CO <sub>2</sub> emissions rate (tons/MWh)	0.0584	0.5600

TABLE II  
INVESTMENT PARAMETERS FOR DISCRETE DERs

Item	Wind turbine	CHP-ICE
Minimum Size (MW)	1	1
Capital cost (M\$/MW)	2.64	3.074
Operation cost (M\$/MWh)	0.000017	0.000145
Heat-to-power recovery ratio	-	1.019
Lifetime (years)	20	20
CO <sub>2</sub> emissions rate (tons/MWh)	0.0276	0.5600

#### B. Scenario Generation

Based on the HMM method, the scenarios of uncertainty matrix are generated using the historical WT/PV generation and electricity/heating demand [17]. As shown in Fig. 4, the moment errors between the generated scenarios and historical scenarios reduce significantly, as the number of scenarios increase from 10 to 100. Hence, the generated scenarios effectively capture the stochasticity of historical data. Thereafter, the minimum number of scenarios, providing the best trade-off between computational accuracy and efficiency, are determined by comparing the objective function value and computation time against the number of scenarios [15]. As shown in Fig. 5, the objective (Case II) converges as the number of scenarios reaches 80. Thereafter, the computation time increases without changing the objective function value. Thus, 80 scenarios are sufficient for the MMIP solution.

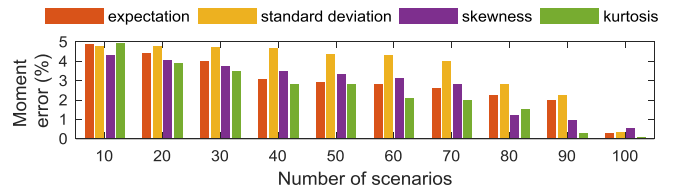


Fig. 4. Moment errors between generated scenarios and historical scenarios

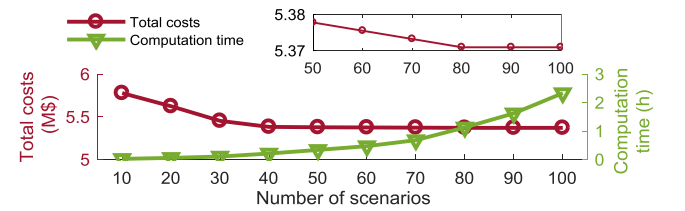


Fig. 5. Selection of scenarios for the solution of MMIP problem (Case II)

#### C. Numerical Results

The MMIP solution (Table III) presents the optimal DER capacities at each bus (e.g. b1, b2 etc.), the annualized cost of investment, operation and unsupplied loads, and the annual CO<sub>2</sub> emissions. In Case I, 4 MW of CHP-ICEs and 0.1 MW of gas boiler are installed to meet the electricity and heating demand, without investment in the wind turbines or photovoltaics. In Case II, which considers the composite cost/emission objective, 2 MW of WTs and 1.2 MW of PVs are allocated. Moreover, the total boiler capacity increases to 3 MW compared to Case I, whereas the CHP-ICE capacity remains 4 MW. The optimal DER mix in Case II results in a 13.5% reduction in the CO<sub>2</sub> emissions at the expense of a 10% increase in the total costs, compared to Case I. These results confirm the effectiveness of the proposed model, in terms of significant reductions in the costs and emissions.

TABLE III  
MMIP SOLUTION: OPTIMAL DER MIX, COSTS AND EMISSIONS

Item		Case I	Case II
DER Mix	Photovoltaic (MW)	0	0.4(b9),0.8(b5)
	Wind-turbine (MW)	0	1(b3),1(b13)
	CHP-ICE (MW)	2(b1),1(b2),1(b4)	2(b1),1(b2),1(b4)
	Gas boiler (MW)	0.1(b1)	1.6(b1),1.4(b2)
Costs	Investment (M\$)	1.161	1.940
	Operation (M\$)	3.683	3.431
	Unsupplied load(M\$)	0	0
	<b>Total (M\$)</b>	<b>4.844</b>	<b>5.371</b>
<b>CO<sub>2</sub> emissions (tons)</b>		<b>16,563</b>	<b>14,329</b>

The optimal electricity and heating dispatch in case II for the July and December weekdays are shown in Fig. 6(a) and Fig. 6(b), respectively. Several observations can be made. For the July weekday, the PV output is higher due to the extended day-hours while the wind generation pattern is quite similar, compared to the December weekday. Moreover, the heating demand is lower, thus requiring less output from the CHP-ICE. For the December weekday, the CHP-ICE and boiler outputs pick up to meet the excessive heating demand. Hence, it is demonstrated that the proposed model explicitly utilizes the interplay between the electricity and heating generators to satisfy the demand.

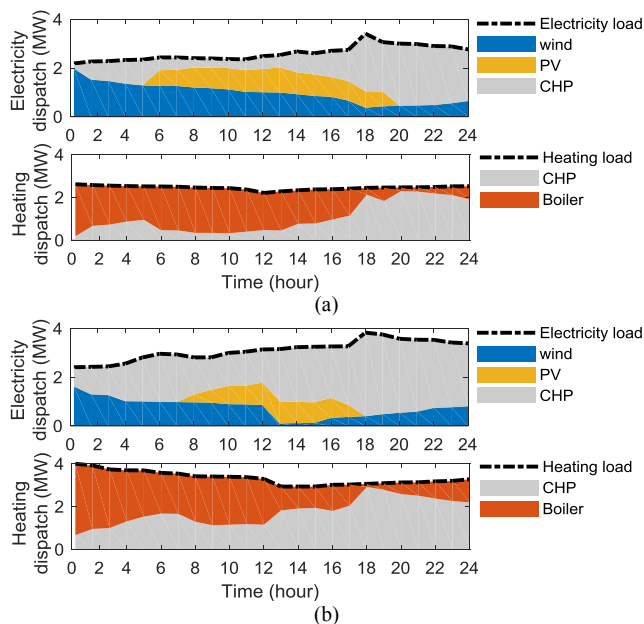


Fig. 6 Optimal electricity and heating dispatch in Case II (a) July weekday (b) December weekday

#### IV. CONCLUSION AND FUTURE WORK

This paper presented a scenario-based stochastic investment planning model for the multi-energy microgrids. The solution determined the optimal distributed energy resource mix, siting and sizing, whilst minimizing the overall microgrid costs and carbon dioxide emissions. The proposed model incorporated an uncertainty matrix to contemplate the operational uncertainties of wind and photovoltaic generation, as well as the electricity and heating demand. The uncertainty matrix was generated via the heuristic moment matching method which effectively captured the stochastic

moments and correlation among the historical data. The effectiveness of the proposed model was confirmed in the 19-bus microgrid test system, in terms of significant reductions in the microgrid costs and CO<sub>2</sub> emissions.

Based on the insights obtained from this work, two research directions are considered worth further research effort. Firstly, a comprehensive planning model should consider the electricity and heating storage systems, in addition to the generation and demand of cooling energy in the multi-energy microgrid. In addition, the efficient integration of plugged-in electric vehicles into the multi-energy microgrid should be further investigated.

#### REFERENCES

- [1] S. Mashayekh *et al.*, "Security-constrained design of isolated multi-energy microgrids," *IEEE Trans. Power Syst.*, vol. 8950, pp. 1–11, 2017.
- [2] A. Ehsan and Q. Yang, "Optimal integration and planning of renewable distributed generation in the power distribution networks: A review of analytical techniques," *Appl. Energy*, vol. 210, pp. 44–59, 2018.
- [3] Z. Wang, B. Chen, J. Wang, J. Kim, and M. M. Begovic, "Robust optimization based optimal dg placement in microgrids," *IEEE Trans. Smart Grid*, vol. 5, no. 5, pp. 2173–2182, Sep. 2014.
- [4] A. Khodaei and M. Shahidehpour, "Microgrid-based co-optimization of generation and transmission planning in power systems," *IEEE Trans. Power Syst.*, vol. 28, no. 2, pp. 1582–1590, 2013.
- [5] D. Singh, D. Singh, and K. S. Verma, "Multiobjective optimization for DG planning with load models," *IEEE Trans. Power Syst.*, vol. 24, no. 1, pp. 427–436, 2009.
- [6] B. Kroposki, P. K. Sen, and K. Malmedal, "Optimum sizing and placement of distributed and renewable energy sources in electric power distribution systems," *IEEE Trans. Ind. Appl.*, vol. 49, no. 6, pp. 2741–2752, 2013.
- [7] A. Omu, R. Choudhary, and A. Boies, "Distributed energy resource system optimisation using mixed integer linear programming," *Energy Policy*, vol. 61, pp. 249–266, 2013.
- [8] J. Keirstead, N. Samsatli, N. Shah, and C. Weber, "The impact of CHP (combined heat and power) planning restrictions on the efficiency of urban energy systems," *Energy*, vol. 41, pp. 93–103, 2012.
- [9] E. D. Mehleri, H. Sarimveis, N. C. Markatos, and L. G. Papageorgiou, "Optimal design and operation of distributed energy systems: Application to Greek residential sector," *Renew. Energy*, vol. 51, pp. 331–342, 2013.
- [10] A. K. Basu, A. Bhattacharya, S. Chowdhury, and S. P. Chowdhury, "Planned scheduling for economic power sharing in a CHP-based micro-grid," *IEEE Trans. Power Syst.*, vol. 27, no. 1, pp. 30–38, 2012.
- [11] K. Hoyland, M. Kaut, and S. W. Wallace, "A heuristic for moment-matching scenario generation," *Comput. Optim. Appl.*, vol. 24, pp. 169–185, 2003.
- [12] J. Lofberg, "YALMIP: A toolbox for modeling and optimization in MATLAB," in *IEEE International Conference on Computer Aided Control Systems Design, Taipei*, 2004, pp. 284–289.
- [13] IBM ILOG CPLEX, "V12. 1: User's manual for CPLEX," 2009.
- [14] J. A. Taylor and F. S. Hover, "Convex models of distribution system reconfiguration," *IEEE Trans. Power Syst.*, vol. 27, no. 3, pp. 1407–1413, 2012.
- [15] S. F. Santos *et al.*, "Novel multi-stage stochastic DG investment planning with recourse," *IEEE Trans. Sustain. Energy*, vol. 8, no. 1, pp. 164–178, 2016.
- [16] S. Mashayekh, M. Stadler, G. Cardoso, and M. Heleno, "A mixed integer linear programming approach for optimal DER portfolio, sizing, and placement in multi-energy microgrids," *Appl. Energy*, vol. 187, pp. 154–168, 2017.
- [17] Electric Reliability Council of Texas, "Generation." [Online]. Available: <http://www.ercot.com/gridinfo/generation>. [Accessed: 03-May-2018].